Solute Diffusion in Lipid Bilayer Membranes: An Atomic Level Study by Molecular Dynamics Simulation

Donna Bassolino-Klimas, Howard E. Alper, and Terry R. Stouch*

Department of Macromolecular Modeling, Bristol-Myers Squibb Pharmaceutical Research Institute, P.O. Box 4000, Princeton, New Jersey 08543

Received May 20, 1993; Revised Manuscript Received August 31, 1993®

ABSTRACT: To elucidate the mechanism of solute diffusion through lipid bilayer membranes, nearly 4 ns of molecular dynamics simulations of solutes in phospholipid bilayers was conducted. The study, the first atomic level study of solute diffusion in a lipid bilayer, involved four simulations of an all-atom representation of a fully solvated dimyristoylphosphatidylcholine (DMPC) bilayer in the Lα phase with benzene molecules as solutes, totaling over 7100 atoms. These simulations agree with experimental evidence that the presence of small solutes does not affect bilayer thickness but does result in slight perturbations in the ordering of the hydrocarbon chains. At room temperature, the benzene molecules have essentially isotropic motion and rotate freely. The rate of translational diffusion varies with position within the bilayer and is faster in the center than near the zwitterionic headgroups and is in excellent agreement with experimental values for the diffusion of small solutes in a bilayer. These simulations have elucidated the mechanism of diffusion in a bilayer to be similar to the "hopping" mechanism found for the diffusion of gases through soft polymers. Jumps of up to 8 Å can occur in as little as 5 ps whereas average motions for that time period are only $\sim$1.5 Å. In many cases, the jumps are moderated by torsional changes in the hydrocarbon chains which serve as "gates" between voids through which the benzene molecules move. Comparison of these simulations with another 1000-ps simulation of benzene in a pure alkane provides evidence that lipid bilayers should not be treated as a homogeneous bulk hydrocarbon phase.

Biomembranes play an integral role in cellular processes. Membrane permeation of small molecules is the basis of passive drug and metabolite uptake. In order to traverse a lipid bilayer membrane, a solute must enter through the polar headgroup region, diffuse within the hydrocarbon region, and then leave through the polar headgroup region on the other side. However, little is known about the mechanism or the rate-determining step of this process at the atomic level. In addition, while the structure and dynamics of lipid membranes are believed to play a vital role in the transport of biomaterials and pharmaceutical agents, little is known about the atomic-level structure and dynamics of these processes because their fluidity makes experimental characterization difficult.

Much of what is known about the diffusion of small molecules through bilayer membranes has been derived from studies of anesthetics. These studies have debated the effect of anesthetics on lipid bilayer membranes in an effort to deduce their mechanism of action. Early theories proposed that the mode of action of anesthetics included membrane expansion (Seeman, 1972; Ashcroft et al., 1977; Haydon et al., 1977). Subsequent studies reported no change in membrane thickness for the concentrations of benzyl alcohol used as local anesthetics (Turner & Oldfield, 1979). Higher concentrations of general anesthetics showed increases in hydrocarbon chain disorder, yet still maintained constant membrane thickness (Franks & Lieb, 1979). More recently, a relationship between the molecular volume of a carboxylic ester and the concentration required for local anesthetic effects was noted (Elliot et al., 1987).

The earliest theories of transport across a membrane date back to studies by Overton (1899), who found that the permeability of a molecule through a membrane correlated with the partition coefficient of that molecule into a hydrophobic solvent. However, some very small molecules permeate faster than predicted by Overton's rule (Cohen, 1975; Finkelstein, 1976; Walter & Gutknecht, 1984). Walter and Gutknecht (1986) also found that the permeability of small nonelectrolytes in membranes was inversely proportional to molecular size. Possible explanations for this behavior include the "soft-polymer" hypothesis which proposes that small solutes fit into holes available in the acyl-chain region of the bilayer and move between holes by a "hopping" mechanism (Lieb & Stein, 1969, 1971; Trauble, 1971). This would require dynamic pockets of free volume into which the solute can enter (Franks & Lieb, 1981). Smaller solutes would require smaller holes and therefore permeate faster.

A number of experimental studies have probed the diffusion of small molecules through lipid membranes. Studies using ^{13}C relaxation experiments showed that the translational motion of small nitroxide solutes in dipalmitoyllecithin liposomes was faster in the center of the bilayer than near the polar interface (Dix et al., 1978). On this basis, permeation through the headgroup region was proposed as the rate-determining step in transport of nonpolar molecules. NMR studies (DeYoung & Dill, 1988) indicated that the partitioning of benzene into DMPC and DPPC lipid bilayers was dependent on the surface density of the bilayer chains. Solute partitioning decreased over an order of magnitude as the surface density was increased from 0.5 to 0.9. These observations are consistent with the thermodynamic theories of Marqussee and Dill (1986). Both studies demonstrate that since bilayers are interfacial phases of matter (i.e., their physical properties vary

* Author to whom correspondence should be addressed.
® Abstract published in *Advance ACS Abstracts,* November 1, 1993.

0006-2960/93/0432-12624$04.00/0 © 1993 American Chemical Society

with distance from the interface), the bilayer should not be treated as a bulk phase.

Recently, there have been a number of theoretical studies of the diffusion of small solutes through biomolecules (Elber & Karplus, 1990; Verkhivker et al., 1992; McKinnon et al., 1992). A time-dependent Hartree–Fock method was proposed to study the diffusion of carbon monoxide molecules through myoglobin via molecular dynamics simulations (Elber & Karplus, 1990). It was noted that the carbon monoxide diffused by hopping between cavities mediated by several side-chain dihedral angles that changed abruptly during the course of the simulation. It was found that motions in the protein backbone coupled with side-chain fluctuations were necessary for the ligands to enter and leave the heme pocket. The protein dynamics played a critical role in diffusion by lowering the energy of activation of a number of pathways by hundreds of kilocalories per mole. In a subsequent study (Verkhivker et al., 1992), the diffusion of carbon monoxide through lupine leghemoglobin was investigated. It was reaffirmed that the protein motions play an important role in the diffusion process, and a two-part model for ligand diffusion was proposed. In another study, nonequilibrium molecular dynamics was used to force oxygen through a hexadecane/cholesterol monolayer during a relatively short simulation (McKinnon et al., 1992). It was shown that increased cholesterol concentration resulted in enhanced diffusion of the oxygen.

Since it has been proposed that the mechanism of diffusion in a bilayer may be similar to that found in polymers, simulations of polymers are also of interest. There have been a number of simulation studies of the diffusion of small molecules in polymers, although CH_4 is the largest penetrant molecule studied to date (Takeuchi & Okazaki, 1990; Takeuchi, 1990a,b; Sonnenburg et al., 1990; Müller-Plathe, 1991, 1992; Müller-Plathe et al., 1992). Early simulation studies by Takeuchi and Okazaki (1990) suggest that the free volume theory for the diffusion of simple liquids (Cohen & Turnbull, 1959) may be applicable to the diffusion of gases through polymers. It was found that the degree of chain flexibility correlated with the calculated diffusion coefficient. In subsequent work (Takeuchi, 1990a,b), a 300-ps molecular dynamics simulation of a spherical molecule in an infinite polymer showed cooperativity between jumps of the solute and chain motions of the polymer.

The results of molecular dynamics simulations of methane in polyethylene (Müller-Plathe, 1991) indicate that permeation proceeds by a hopping mechanism whereby penetrant molecules "hop" between neighboring voids. Subsequent simulations (Müller-Plathe, 1992) of hydrogen and oxygen in amorphous polypropylene also found a hopping motion to be the mechanism of diffusion. Calculated diffusion coefficients agreed within an order of magnitude with experimental results when all-atom models were employed. More recently, computational evidence for anomalous diffusion was found (Müller-Plathe et al., 1992) via several nanosecond simulations of oxygen and helium in polyisobutylene. These studies also showed that the use of a united-atom model artificially raised diffusion rates by almost 2 orders of magnitude compared to experiment and simulations using explicit hydrogen atoms.

More recently, the transport of helium and methane through poly(dimethylsiloxane) (PDMS) was studied via a 300-ps molecular dynamics computer simulation (Sok et al., 1992). A jump mechanism for the diffusion of methane was noted that involved fluctuations in the polymer matrix resulting in transient channels through which solutes could move between holes.

Although a number of simulation studies have attempted to understand lipid bilayer structure and dynamics (Edholm et al., 1983; Van der Ploeg & Berendsen, 1983; Pastor et al., 1991; Jonsson et al., 1986; Watanabe et al., 1988; Scott, 1986; Edholm & Johansson, 1987; Egberts 1988; Egberts & Berendsen, 1988; Scott & Kalaskar, 1989; Berkowitz & Raghaven, 1991; Raghaven et al., 1992; Damodaran et al., 1992; Stouch, 1993; Stouch et al., 1993; Alper et al., 1993a,b), none have addressed diffusion of small molecules in lipid bilayers at the atomic level.

In this study, the first stimulations of small molecule diffusion through a lipid membrane are presented. These studies extend previous molecular dynamics simulations of lipid bilayers (Stouch, 1993; Stouch et al., 1993) and include four simulations of over 7100 atoms totaling 4 ns of simulation time. The initial studies presented here center on benzene, in part because it is nonpolar and because although it is larger than solute studies in previous simulations of diffusion, it is still relatively small and simple and is of a size relevant to other membrane solutes, including drugs.

METHODS

The starting bilayer model was obtained by extracting a single configuration from a well-equilibrated simulation of a fully hydrated lipid bilayer (Stouch, 1993; T. R. Stouch, unpublished results). The details of the models and the simulations were described elsewhere (Stouch, 1993). Briefly, the system consisted of 36 dimyristoylphosphatidylcholine (DMPC) lipid molecules arranged into two monolayers (18 in each layer) with lateral dimensions of 34.5 Å × 34.5 Å in the x–z plane, solvated with 962 water molecules (481 above/below each layer), totaling 7134 atoms. Two-dimensional periodic boundary conditions were employed in the x–z plane to simulate an infinite bilayer. Repulsive walls were used to contain the water in the y direction at the appropriate density, resulting in an effective "y" dimension of 61 Å (Stouch, 1993; Alper et al., 1993a).

All simulations were performed with a heavily modified version of DISCOVER (Biosym Technologies, Inc.) and were run on a Cray Y-MP 2E/2-32. An all-atom representation of all molecules (lipids, waters, and benzene), including all hydrogen atoms, was employed. It has been shown (Müller-Plathe et al., 1992) that a united-atom model results in artificially high diffusion rates and is therefore inappropriate for studying diffusion. Other studies (Williams, 1967; Ryckaert & Klein, 1986; Rychaert et al., 1989) on n-alkanes strongly suggest that all hydrogen atoms must be included to reproduce experimental data. The force field for the lipids was described previously (Stouch et al., 1991; Williams & Stouch, 1993) with the exception that the 1,4 interactions were scaled by 0.6 (T. R. Stouch, unpublished results). A flexible three-center SPC-like (Berendsen et al., 1981) water model was used which has been characterized to be in good agreement with both experiment and the computed properties of other water potentials (K. Lau, H. E. Alper, T. Thacher, and T. R. Stouch, unpublished results). For benzene, the CVFF force field (Biosym Technologies, Inc.) (Hagler et al., 1979; Dauber-Osguthorpe et al., 1988) was employed with partial charges of $qc = -0.1$ and $qh = 0.1$ used for the carbons and hydrogens in benzene, respectively.

The Verlet (1967) algorithm was used to integrate the equations of motion with a time step of 1 fs. The temperature was maintained at 320 ± 3 K for all simulations by coupling the system to an external bath (Berendsen et al., 1984). This

Table I: Summary of Simulations of Benzene in a DMPC Bilayer

system	total time (ps)	equilibration time (ps)	no. of benzenes
BZ1	525	25	1
BZ2	1000	195	1
BZ3	1100	90	1
BZ4	1100	90	4

is well above the gel → Lα transition temperature (24 °C) for DMPC bilayers (Ladbrooke & Chapman, 1969).

The nonbonded neighbor list was updated every 20 time steps and evaluated to a distance 2 Å longer than the cutoff. This 2-Å "buffer" additionally ensures that atoms do not frequently move across the cutoff boundary. A nominal 10-Å cutoff was used for all interactions in all simulations. For interactions between the waters, hydrocarbon chains, benzene molecules, and the glycerol moieties, nonbonded cutoffs were applied between small neutral groups of atoms (i.e., a "group"-based cutoff) as described previously (Stouch et al., 1991; Alper et al., 1993a). A "residue"-based cutoff was employed for all interactions involving the zwitterionic phosphocholine headgroup, such that the whole group was treated as a single neutral moiety as described in Alper et al. (1993a). This results in a larger effective cutoff for the headgroups (approximately 16 Å) which has been shown to be important for electrostatic interactions (Alper et al., 1993a). Since the use of switching functions may disrupt the potentials and forces in a nonphysical way (Alper & Levy, 1989; Smith & Pettitt, 1991; Alper et al., 1993a) and introduce artifacts into the simulation properties, switching functions were not employed in any of the simulations.

The benzene molecules were manually introduced into voids in the hydrocarbon region of the bilayer. The systems were then minimized to reduce any residual unfavorable steric interactions. The systems were then heated to 320 K over 10 ps and equilibrated for another 25–195 ps. Thereafter, data was collected every 100 fs for analysis.

A total of four simulations are discussed in this paper (see Table I). Simulations BZ1, BZ2, and BZ3 each contained a single benzene. Simulation BZ4 contained four benzene molecules (A, B, C, and D) to investigate the effects of increased benzene concentration as well as to improve statistics on the benzene-related properties. The first simulation was run for 500 ps while the others were run for over 1000 ps each (see Table I). Simulations of this duration have been shown to be necessary to obtain proper convergence of the bilayer properties to the appropriate experimental values (Stouch, 1993; Stouch et al., 1993).

Simulations of benzene in pure hydrocarbon were performed to study the effect of the chain orientation within the bilayer on the benzene diffusion properties. A total of 72 tetradecane molecules (corresponding to 2 from each of 36 DMPC molecules) were put in a box (34.5 Å × 26.0 Å × 34.5 Å) designed to be the same size as the hydrocarbon region of the bilayer. Coincidentally, although not by design, the density of this box (0.76 g/cm^2) is quite close to that of liquid tetradecane at 300 K (0.76 g/cm^2), allowing comparison to be made between the bilayer and neat alkane. Although conditions were chosen to be essentially identical to those of the hydrocarbon chains in the bilayer, unlike in the bilayer the tetradecane chains were free to reorient in all directions and were not hindered at one end as they would be in a lipid molecule. Three-dimensional periodic boundaries were employed to simulate an infinite box. To allow for rapid torsional isomerization, the torsional potential and the 1–4 nonbonded interaction potential were scaled by 0.1 for 20 ps of molecular dynamics. The full potential was used after this point. A single benzene was then added to a void near the center of the system. The system was minimized and heated as described for the bilayer and then equilibrated for 50 ps. The run was continued for 1 ns during which time data was collected every 100 fs for analysis.

The simulations of benzene in the bilayer took on average 1.66 s/step on a Cray Y-MP/3E-32. The simulations of benzene in the hydrocarbon took 0.90 s/step. These calculations represent approximately 100 CPU days of computer time.

RESULTS AND DISCUSSION

Bilayer Structure. A snapshot of simulation BZ4 is shown in Figure 1. Analysis of the effect of benzene on the structure and dynamics of the lipid bilayer was investigated by comparing the simulations with increasing benzene concentrations to an identical system without any solute (Stouch, 1993; Stouch et al., 1993). Bilayer thickness, measured as the distance between the mean positions of the carbonyl carbons of each monolayer, was averaged over all time steps in the simulations (Table II). For all four simulations (no benzene, two with one benzene, and one with four benzene molecules), these average values were within one standard deviation of each other and well within the spontaneous fluctuation of this quantity, which is on the order of several angstroms. These results indicate that benzene in low concentrations has little effect on the gross structure of the bilayer. Although early theories suggested that anesthetics elicited their response by disrupting membrane structure, X-ray scattering studies failed to detect changes in membrane thickness at clinical concentrations of these substances (Franks & Lieb, 1979). A similar lack of perturbation was observed experimentally for benzyl alcohol in a lipid bilayer at essentially equivalent concentrations (Turner & Oldfield, 1979). In that study, no change in thickness was observed until very high concentrations (approximately three to ten solute molecules per lipid molecule) of benzyl alcohol were added. NMR studies also found that the addition of similar concentrations of hexane to a DMPC bilayer left the bilayer intact (Jacobs & White, 1984). These simulations provide additional evidence that clinical concentrations of small solutes have no effect on bilayer thickness. Although this large-scale property remains unchanged, slight changes in the structure and dynamics of the bilayer were evidenced. The presence of the benzene molecules resulted in a small decrease in the number of hydrocarbon torsions residing in the gauche conformation. In addition, the rate of torsional interconversion decreased very slightly with the presence of benzene.

Another way that changes in structure and dynamics can be discerned is by examining the order parameters. Figure 2 shows a plot of the order parameters of the methylene groups of the hydrocarbon chains for a bilayer without solute and the bilayer with the various concentrations of benzene. In this figure, a value of 1 indicates that the chains are all-trans and perpendicular to the bilayer plane, –0.5 indicates that they are all-trans and parallel to the plane, and 0 indicates random orientation. It is well-known that the methylene groups higher up in the chain (positions 2, 3, 4, ...) are more ordered than the methylenes at the ends of the chain near the center of the bilayer (positions 10, 11, 12) (Seelig & Seelig, 1980; Dill & Flory, 1980). The trends in the simulations presented here are slight but noticeable. The values presented are converged to a precision of ~0.001 unit. Errors on the order of 0.01 unit

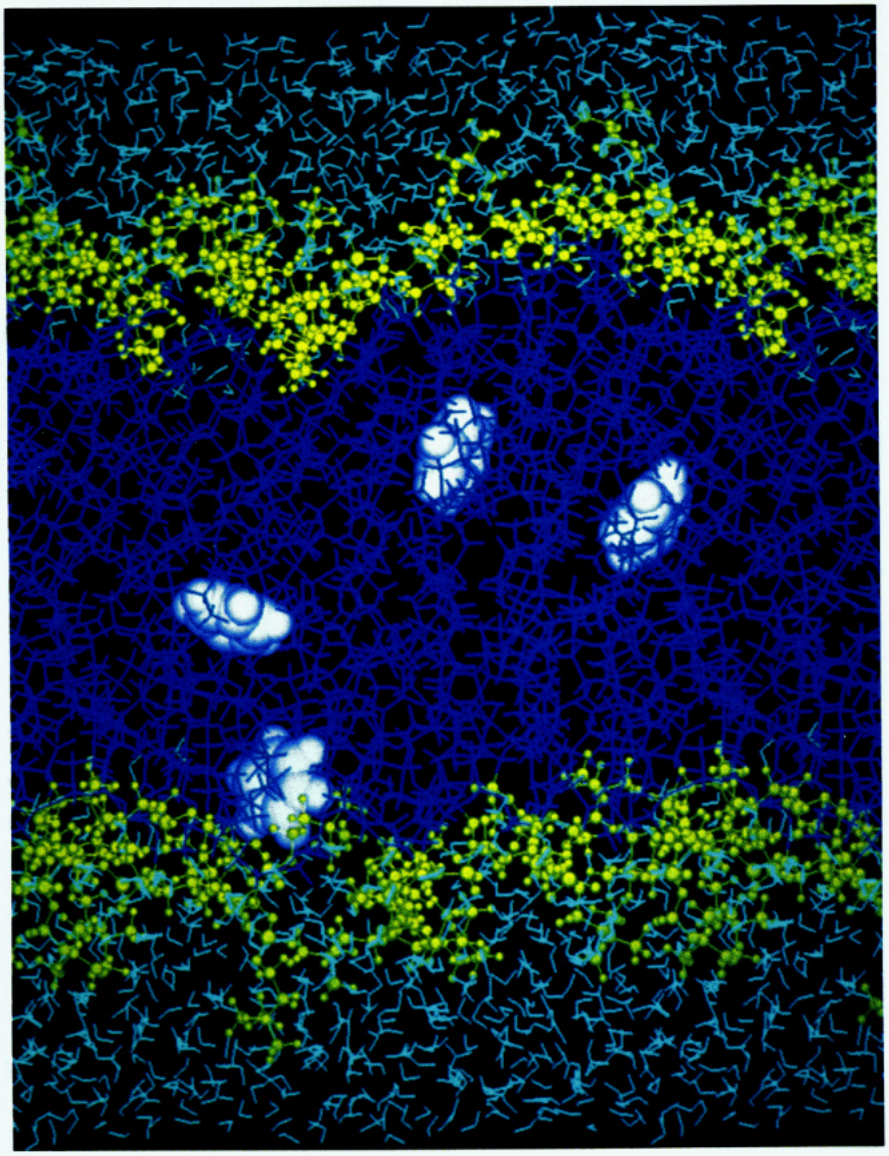

FIGURE 1: Snapshot of one configuration from simulation BZ4. The benzene molecules are shown in white as CPK models, the atoms in the headgroups in yellow, the hydrocarbon chains in dark blue, and the water molecules in cyan.

Table II: Thickness of Hydrocarbon Region[a]

run	mean (Å)	SD
S0[b]	25.3	0.3
BZ2	25.3	0.2
BZ3	25.5	0.2
BZ4	25.4	0.2

[a] Mean distance between the mean positions of each monolayer's carbonyl carbons. [b] S0 is the simulation without any solute; see text.

were derived by dividing the simulation into two halves and calculating the order parameters for each half. Toward the carbonyl groups (positions 2, 3, 4, ...) there is a decrease in order that parallels increasing concentration. In the middle of the chain, the results are mixed. At the end of the chain, the different simulations are almost identical. As will be discussed below, the center of the bilayer has more "free space" than the headgroup region (Stouch et al., 1993). These results suggest that the benzene molecules can easily fit within already available free space present at the center of the bilayer and so cause little effect on the ordering of the chains. Toward the carbonyl end of the chains, however, less free space is available and the presence of the benzene molecule is felt more strongly, resulting in the noticeable decrease in ordering of the chains.

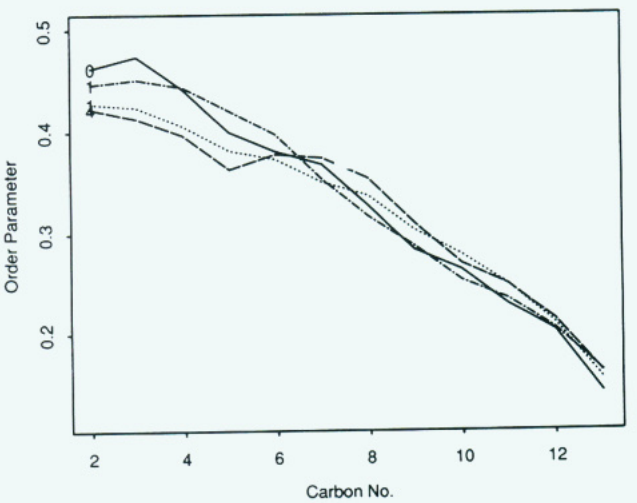

FIGURE 2: Order parameters for simulations with increasing benzene: (—) no benzene (0); (···) BZ2 (1), one benzene; (– • –) BZ3 (1), one benzene; (- - -) BZ4 (4), four benzenes.

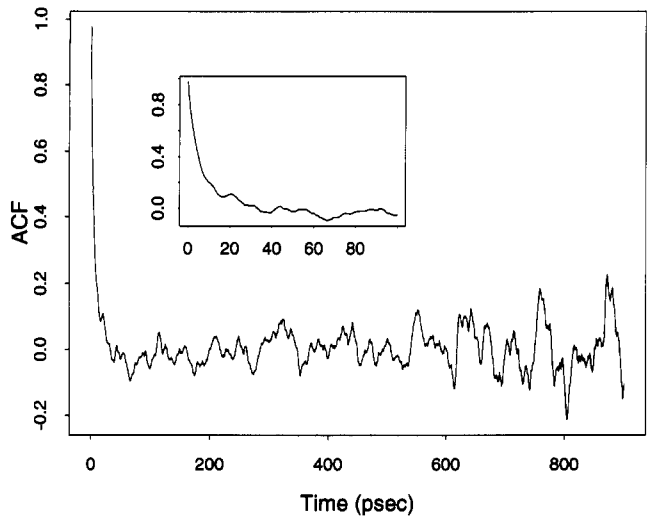

FIGURE 3: Reorientation autocorrelation function of BZ4A (expectation value of the first Legandre polynomial for the C1 → C4 vector). This function was essentially identical for all of the other benzene molecules.

These observations are consistent with early NMR studies involving the anesthetic benzyl alcohol that showed a slight decrease in chain order with increasing concentration of benzyl alcohol (Turner & Oldfield, 1979). Fluorescence polarization experiments later confirmed that lipid order parameters were reduced by 4–8% by the addition of higher concentrations of benzyl alcohol (Carriere & LeGrimmellec, 1986). Similarly, this is consistent with the small decreases in lipid chain order observed from NMR studies of hexane in a DMPC bilayer (Jacobs & White, 1984) and the decrease in lipid bilayer order with increasing concentrations of the local anesthetics carbisocaine and lidocaine (Hianik et al., 1990). Thus, although at these concentrations no gross changes in bilayer morphology are seen, slight changes in the order and dynamics of the bilayer interior are found.

Benzene Reorientation. The reorientational correlation time (τ_r) of the benzene molecules was calculated using the vector between two carbon atoms at opposing sides of the benzene ring. Figure 3 shows this function for BZ4A and provides a reorientational correlation time of ≈25 ps. This agrees with experimentally determined correlation times for other small molecules in bilayers. Dix estimated τ_r to be 20 ps (Dix et al., 1978) for di-*tert*-butyl nitroxide, a molecule of similar size, in diplamitoyllecithin bilayers at 323 K.

Each of the seven benzene molecules had essentially equivalent reorientational correlation functions and reorientational correlation times. This is despite the fact that, as will be shown, the benzene molecules tend to sample different regions of the bilayer differently.

The angle formed between the same benzene vector and the vector normal to the bilayer plane over the time course of the simulation indicates that the benzene molecules rotated freely and experienced no favored orientation.

The ranges of each of the benzenes' center-of-mass coordinates in x, y, and z Cartesian directions are given in Table III. In several cases the movement of the benzene molecules was essentially isotropic (BZ1, BZ2, and BZ4A). In the others, a wider range might have been sampled in one or two directions; however, no pattern suggesting a preferred direction of movement was present. In particular, there was no evidence of preferred motion perpendicular to the bilayer plane (i.e., parallel to the hydrocarbon chains).

As one moves from the outside of the bilayer to the inside, one traverses several distinct regions, i.e., (1) the polar headgroup/water interface region, (2) the carbonyl region of the headgroups (3) the nonpolar hydrocarbon chain region, and (4) the center where the terminal methyls of opposing bilayers meet. Figure 4 traces the center-of-mass of each benzene through the trajectory in the direction perpendicular of the plane of the bilayer. It shows that the different benzene molecules moved freely between regions of the bilayer. Despite this free motion, BZ1, BZ4C, and BZ4D spent most of the simulation time moving in the general region of the center of the bilayer near the terminal methyls. BZ3 and BZ4B spent more time near the carbonyl region of the headgroups than other regions. BZ2 and BZ4A sampled several regions equally. For future discussions the benzenes will be referred to as "residing" in these regions in which they spend the most time. Figure 4c traces the path of BZ4D in three dimensions throughout its entire trajectory. This figure illustrates that BZ4D moved freely from one region of the bilayer to another. The color varies with the time of the trajectory and shows that the benzene explored several locations and did not simply rattle around in one void or move back and forth between voids. This sort of behavior has been predicted by statistical mechanics theories of solute distribution in bilayers (Marqussee & Dill, 1986).

Diffusion of Solutes through a Bilayer. Diffusion coefficients, calculated from the mean squared displacements of each molecule over all possible time origins ($<|R(t)-R(0)|^2>$), are reported in Table III. Note that they vary with position in the bilayer. Those benzene molecules that spent a large fraction of their time in the center of the hydrocarbon region (BZ1, BZ4C, and BZ4D) diffused 2–4 times faster than the benzene molecules that spent more time closer to the headgroup regions (BZ2, BZ3, BZ4A, and BZ4B). Although the experimental diffusion coefficient for benzene in a DMPC bilayer is not available, the values are in excellent agreement with those obtained from ^{13}C NMR spin relaxation experiments (Dix et al., 1978) for other small solutes which estimated the diffusion coefficient for di-*tert*-butyl nitroxide in dipalmitoyllecithin to range from 0.5×10^{-6} to 2.0×10^{-6} cm^2/s, depending on location in the bilayer.

Important considerations in the evaluation of the values of properties calculated from simulations are the degree of convergence and the estimates of error for those properties. In order to compare the diffusion coefficients of individual

Table III: Benzene Diffusion Data

	BZ1	BZ2	BZ3	BZ4A	BZ4B	BZ4C	BZ4D	BZ/HC
length (ps)[a]	500	800	1000	1000	1000	1000	1000	1000
x-range (Å)	12.6	8.6	18.6	13.1	14.2	18.6	19.0	8.6
y-range (Å)	11.8	12.2	7.5	13.0	11.2	10.7	11.6	16.8
z-range (Å)	13.2	10.7	9.0	9.8	9.0	27.4	16.1	8.2
diffusion ($\times 10^6$ cm^2/s)	4.0	2.7	1.4	2.1	1.3	3.8	4.6	1.9
most common location	CH_3[b]	c	C=O[b]	c	C=O[b]	CH_3[b]	CH_3[b]	

[a] Length refers to the number of picoseconds used in the analysis. [b] CH_3 resides in center of bilayer. C=O resides near carbonyl or headgroup regions. [c] Moves between different regions equally.

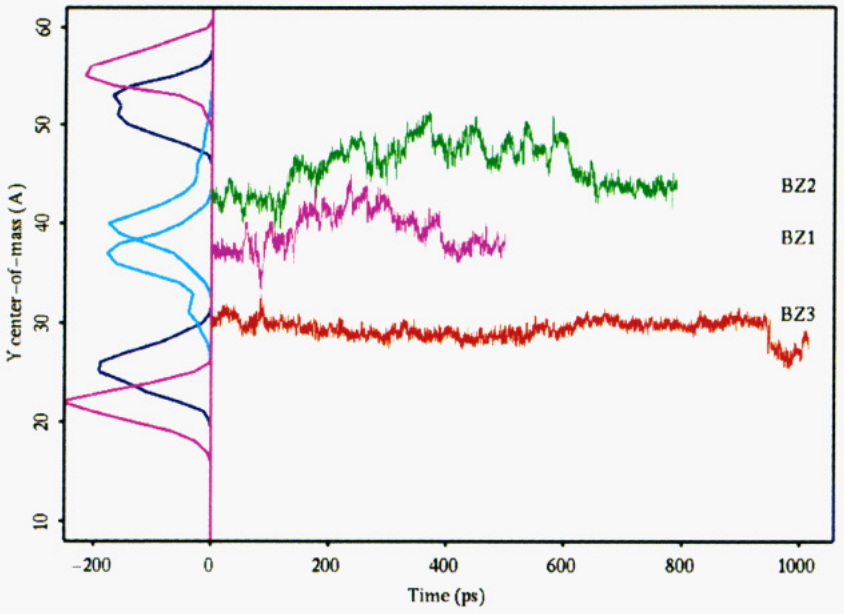

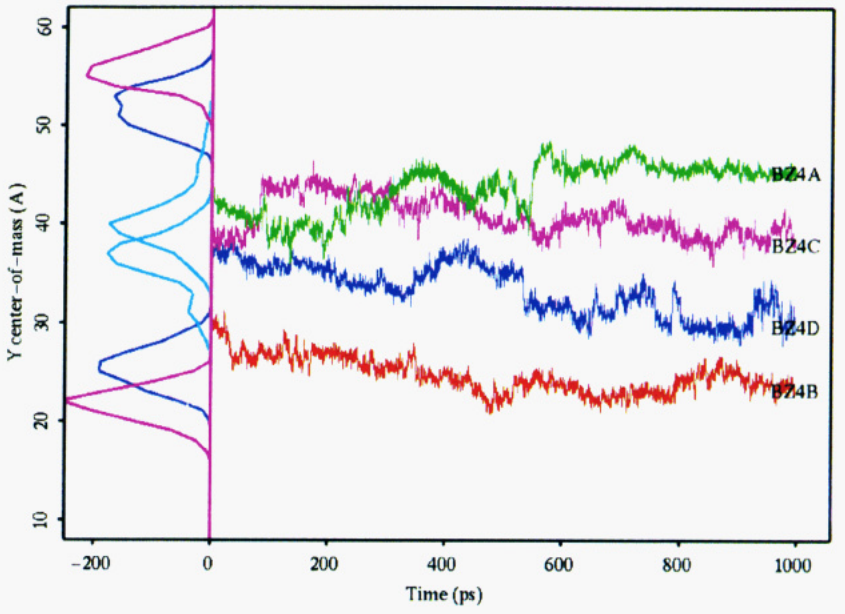

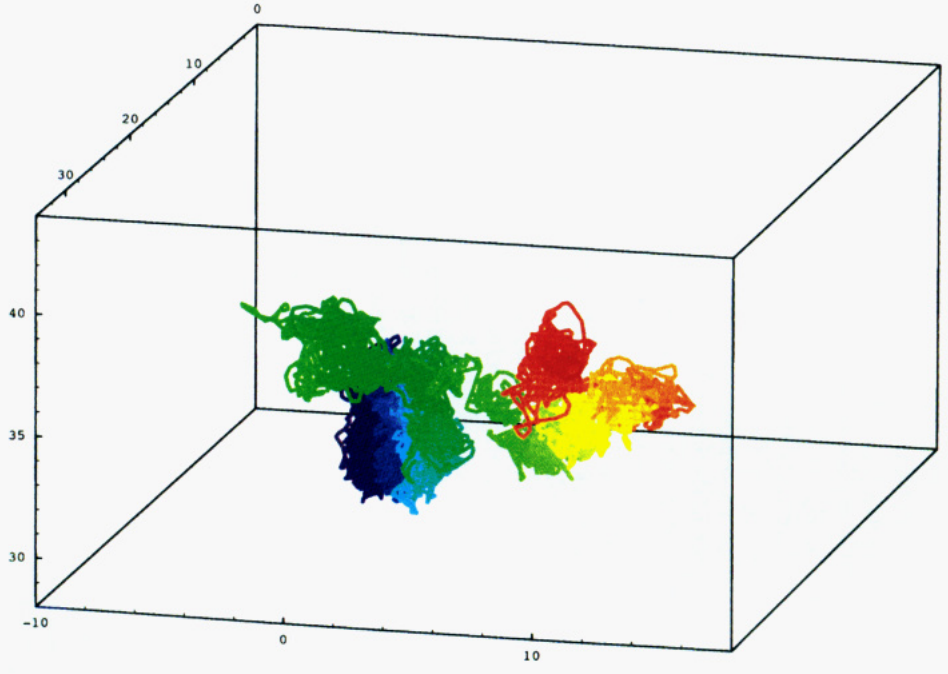

FIGURE 4: *Y* center-of-mass coordinates for (a, top left) each of the benzenes in simulations BZ1, BZ2, and BZ3 and (b, top right) each of the four benzenes in simulation BZ4. The profiles on the left show the probability distributions for atoms of the phospholipids: the phosphate atoms (magenta), the carbonyl atom of chain 1 (dark blue), and carbon-14 of hydrocarbon chain 1 (cyan). (c, bottom left) Trace of the center of mass of BZ4D for the entire trajectory. Colors of the spectrum correspond to simulation time: red is early in the simulation; indigo, at the end. The box outline represents the range of motion of this benzene and is only a fraction of the volume of the entire simulation box.

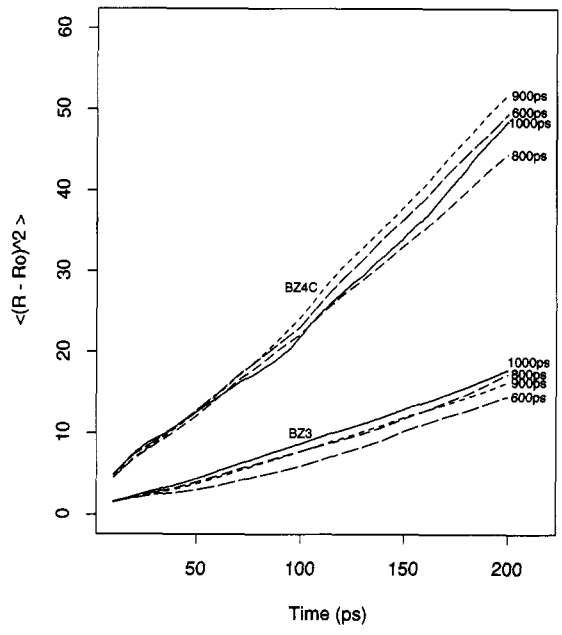

FIGURE 5: Convergence of the mean squared displacement (for the calculation of diffusion) for BZ3 (lower group of lines) and BZ4C (upper group of lines); see text.

benzene molecules, the validity of that comparison was established in two ways. Error estimates for the diffusion coefficients were determined by dividing the trajectories of two of the runs in half, calculating the coefficients for each half, and comparing that value to the mean (which, in both cases, was very close to the value calculated using the entire trajectory). In these cases, the deviations were either 20% or 30%. Previous studies showed that 800–900 ps were required to achieve convergence of many structural properties of membranes (Stouch, 1993; T. R. Stouch, unpublished results; Stouch et al., 1993). Since this property requires as much as 1 ns to converge, and dividing the trajectories in two gave either 400- or 500-ps segments for the error estimate calculation, these error estimates are probably high. Regardless of this, the differences of the values that are compared below are greater than this error estimate. As a further example of the uniqueness of, error estimates for, and convergence of the values of the diffusion coefficients for the individual benzene molecules, note that the calculated coefficients for those molecules residing in different regions of the bilayer were unambiguously different. To illustrate this, Figure 5 shows the mean squared displacement plots for BZ3 and BZ4C at different points along the trajectory. BZ3 spent most of its time in the carbonyl region. The value of its diffusion coefficient, as determined from the slope of these lines, fluctuated between 1.2×10^{-6} and 1.48×10^{-6} cm^2/s. The values for BZ4C, which resides mostly in the bilayer center, range between 3.2×10^{-6} and 4.2×10^{-6} cm^2/s. Although the diffusion coefficients converge slowly, the values for the benzene molecules residing in the different regions of the bilayer do not overlap at any point in the trajectory. The ranges shown by Figure 5 further substantiate the less than 20–30% error estimates for the diffusion coefficients provided by analysis of subsets of the trajectories.

Dix et al. (1978) used ^{13}C NMR spin relaxation experiments to measure gradients in the diffusion tensor across the bilayer using spin-labeled di-*tert*-butyl nitroxide (DTBN) to provide evidence that diffusion does indeed increase with distance from the headgroup region for small solutes. In fact, on the basis of their results they predicted a factor of 2–3 increase in the diffusion coefficient between the carbonyl region of the bilayer and the terminal methyl region, in good agreement with the results of this simulation study presented here. Similarly, they found that the motion of the hydrocarbon chains themselves was less near the interface than near the center (Hubbell & McConnell, 1971; Seelig & Seelig, 1974).

Although in the past biological membranes and the membrane water interface have been equated to bulk hydrocarbon and the interface between organic fluids and water, this supposition, recently challenged by theory and experiment (Dix et al., 1978; DeYoung & Dill, 1988), is further challenged by the results of these simulations. These results show that not only is the headgroup region distinct from the hydrocarbon region but that the hydrocarbon region itself is not homogeneous.

These analyses showed that the long simulations presented in this study were able to reproduce many experimentally derived quantities and encouraged the use of these simulations to explore the mechanism by which the diffusional process occurs.

Mechanism of Diffusion. Much has been speculated about the mechanism of diffusion of small solutes in lipid membranes. Early theories related permeation and diffusion of solutes in lipid membranes to their partition coefficients between oil and water (Overton, 1899). However, it was found that many small molecules permeated and diffused faster than predicted by the Overton rule. A number of theories have been proposed to explain the "extra" permeability. One such proposal (Lieb & Stein, 1969) was that small solutes hop between neighboring voids, similar to that proposed for the diffusion of gas penetrants through polymers (Cohen & Turnbull, 1959). This theory was supported by experimental studies that found that permeability and diffusion were inversely proportional to molecular size for small nonpolar solutes (Walter & Gutknecht, 1986). Presumably, smaller solutes require smaller holes and smaller holes are more probable than larger holes, thereby increasing the diffusion rates of smaller molecules.

It is well-known that there is a large amount of free volume present in lipid bilayers (Dill & Flory, 1980). Studies of free volume within the bilayer show that the frequency and size of voids increase with proximity to the bilayer center (Dill & Flory, 1980; Stouch et al., 1993). This agrees well with the NMR-derived order parameters which show not only a gradual decrease in order with distance from the headgroup region but a large decrease at the center of the bilayer (Seelig & Seelig, 1980). A decrease in density at the bilayer center has also been clearly established from X-ray scattering studies. It is well-known that, in most cases, the hydrocarbon chains from opposing monolayers interdigitate very little (Franks, 1976). All of this suggests that holes through which solutes can move are most numerous in the center of the bilayer. That the diffusion coefficients for benzene molecules in the bilayer center are faster than those at other locations supports Lieb's proposed mechanism, i.e., that solutes are jumping between holes much as is found in polymers (Lieb & Stein, 1969).

Three different quantities aid in understanding the mechanism of diffusion. Figure 6 shows benzene molecule's displacement from its initial position over time ($(R(t) - R(t = 0))^2$). Although all the benzene molecules move substantially, it is evident that some of the benzene molecules move further from their starting point than others, namely, BZ4C and BZ4D, those near the center of the bilayer. The movements are not uniform in either magnitude or time. On occasion, displacements above the average in magnitude, "jumps", occur in a relatively short span of time. To better quantitate the magnitudes and time scales of the displacements,

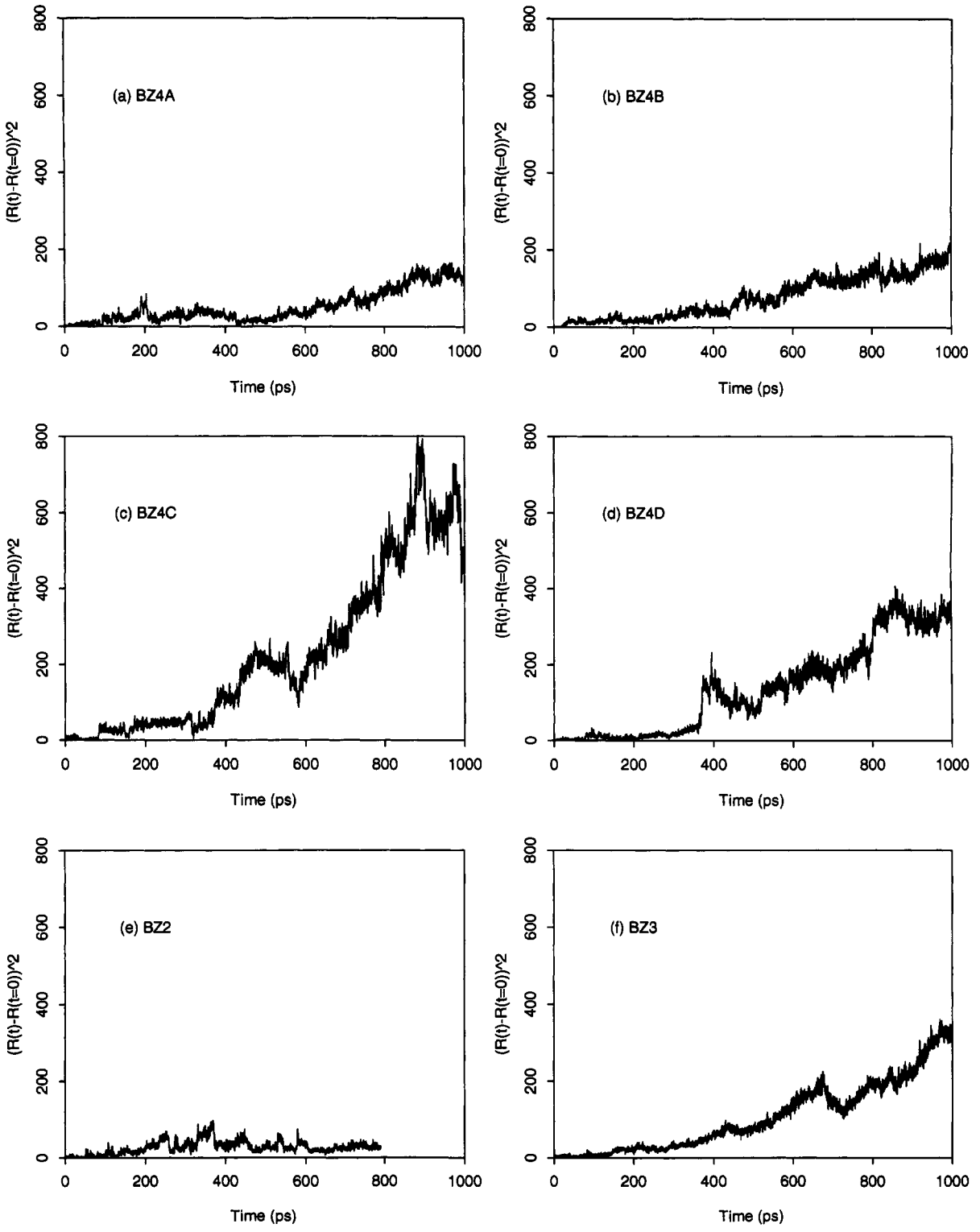

FIGURE 6: Displacements of each of the benzene molecules from their original starting position ($(R(t) - R(0))^2$): (a) BZ4A; (b) BZ4B; (c) BZ4C; (d) BZ4D; (e) BZ2; (f) BZ3.

the distributions of the magnitudes of the motions over 1, 2, 5, 10, 20, 80, and 200 ps were examined and showed that the jumps observed in Figure 6 correspond to motions of 5–8 Å and can occur in as little as 5 ps.

Figure 7 shows the actual distances moved in 5 ps for all possible 5-ps intervals for the different benzene molecules. Spikes occur in the plots for all molecules, showing jumps of 3–7 Å. The benzenes near the bilayer center, BZ4C and BZ4D, exhibit larger and more frequent spikes than those near the headgroup region (BZ3 and BZ4B). Figure 8 shows the distribution of the magnitudes of the motions that occur in 10 ps. The probabilities peak between and 1 and 2 Å, but those benzene molecules in the center (BZ4C and BZ4D) have non-zero probabilities of moving even more than 3 Å and, in fact, show movements as large as 8 Å. This profile changes only incrementally at longer times. In other words, jumps much larger than 7–8 Å do not seem to occur. Of course, movements larger than this occur at long times (>80 ps), but these are probably due to either multiple jumps or jumps combined with other smaller moves. These plots indicate that the benzene molecules "rattle" around in a particular void for a relatively long period of time and

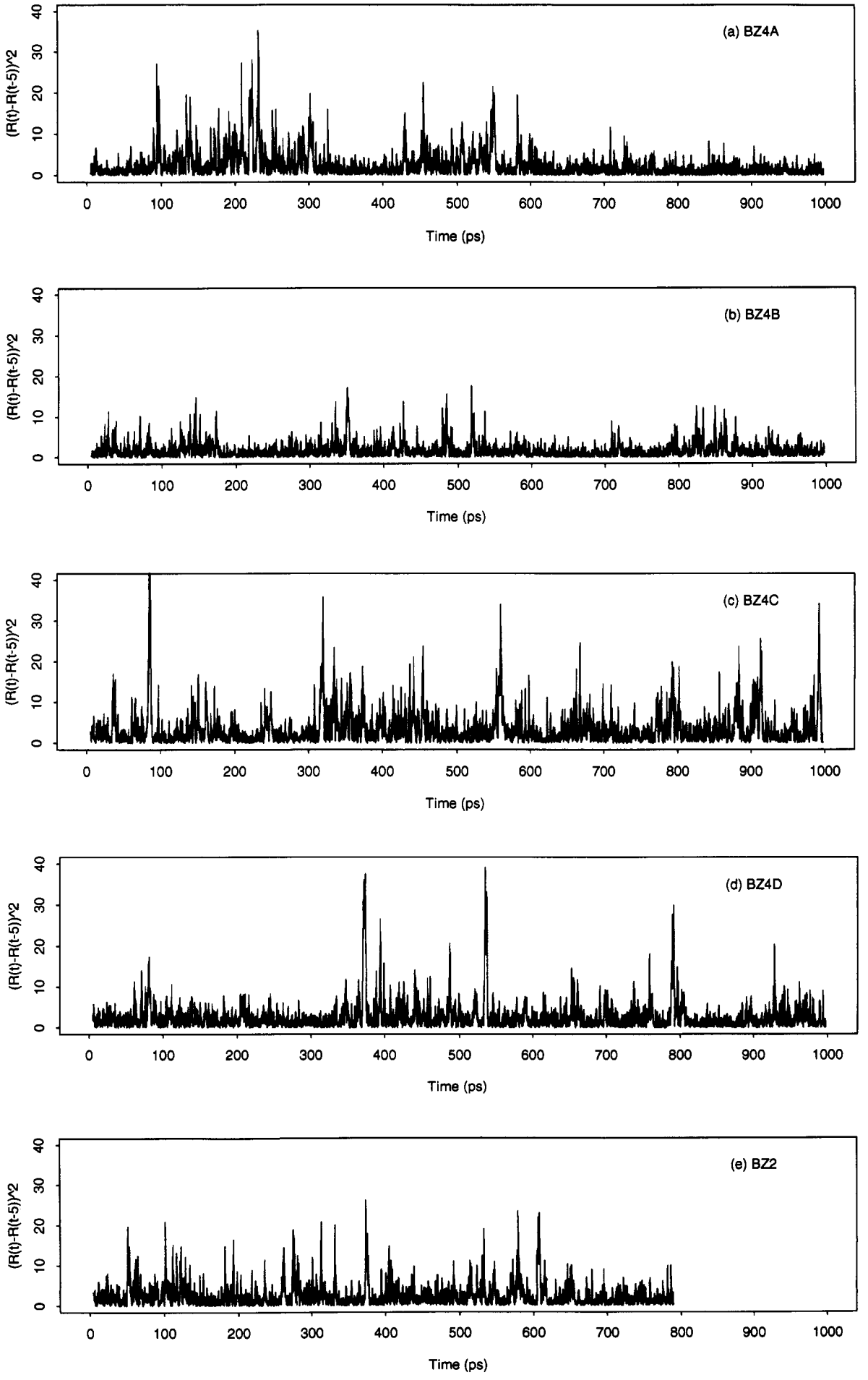
(a) BZ4A
(b) BZ4B
(c) BZ4C
(d) BZ4D
(e) BZ2
(R(t)-R(t-5))^2
Time (ps)
0
10
20
30
40
0
100
200
300
400
500
600
700
800
900
1000

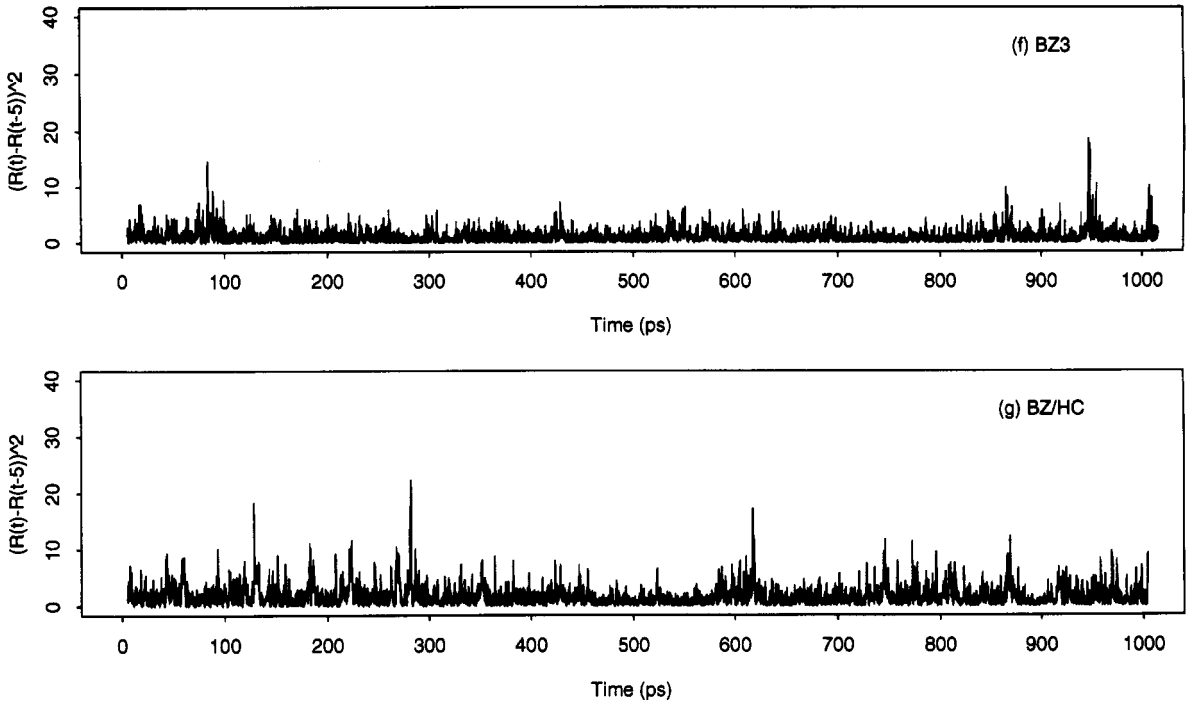

FIGURE 7: Distance moved in a 5-ps interval, calculated for all starting points for (a) BZ4A, (b) BZ4B, (c) BZ4C, (d) BZ4D, (e) BZ2, (f) BZ3, and (g) benzene in pure hydrocarbon.

infrequently take jumps to another void.

The profiles shown in Figures 7 and 8 are characteristic for the benzene molecules in different regions of the bilayer. Both in the simulations presented here and in succeeding simulations at varying temperature, the location of the benzene molecules can be determined from examination of these plots.

The frequency of the jumps is greater for benzene molecules in the bilayer center where the voids are larger and more numerous. In addition, the rate of torsional isomerization has been found from experiment (Seelig & Seelig, 1980) and simulation (Stouch, 1993; T. R. Stouch, unpublished results) to be ≈10 ps in the bilayer center in contrast to the torsions higher up in the chain that have residence times as long as hundreds of picoseconds. This suggests that the infrequent jumps are tied to only one other infrequent event, hydrocarbon chain torsional isomerization. On occasion, a torsional event occurs, which moves a hydrocarbon chain out the path of a benzene molecule and allows the benzene to pass to the next hydrocarbon chain, ≈6–8 Å distant. Note that the size of the larger jumps, 6–8 Å, is the same as the average distance between neighboring hydrocarbon chains (T. R. Stouch, unpublished results).

Detailed analysis of the simulation trajectories illustrates this for BZ4D, which took a large jump between 558 and 569 ps (see Figures 4 and 6). Three torsion angles of two of the lipid chains surrounding this benzene were monitored and are shown in Figure 9. It is clear from Figure 9a that a torsion of one chain abruptly switched from gauche to trans just before the jump occurred at ≈560 ps. It is interesting to note that there were temporary concerted changes in two torsions on another chain (Figure 9b,c). Thus, it appears that two torsions on one chain adjusted temporarily and allowed isomerization of the torsion in the neighboring chain. This transition allowed the benzene molecule to make a rapid change of location. Different stages of this transition are shown in Figure 10.

While it is clear that this process occurred frequently, for some jumps other similar concurrent changes in neighboring torsions were not as obvious, and no doubt lateral motions of the DMPC chains can also play a role in large benzene motions.

Despite the fact that the benzene molecules near the headgroup region diffuse at a significant rate, few jumps were observed, and the residence time between jumps was much longer. This is in agreement with the longer times for torsional isomerization in this region. In addition, the diffusion of these benzene molecules is affected by the increase in density and the increased order of the hydrocarbon chains in this region.

Comparison to Benzene in Unoriented Pure Alkane. It is clear from experiment and simulation that bulk hydrocarbon is not a good model for biomembranes. It is not even clear that bulk hydrocarbon is a good approximation of the hydrocarbon interior (Marqussee & Dill, 1986). In order to more thoroughly explore the role the structure of the membrane plays in the diffusion of the benzene, the comparison study of benzene in a pure unoriented alkane was performed. The calculated diffusion coefficient for the benzene in the unoriented box of tetradecane, given in Table III, is intermediate in value between those residing mostly near the headgroups and those residing mostly near the terminal methyls. The benzene molecules in pure hydrocarbon diffuse slower than benzene molecules near the terminal methyls in the bilayer and faster than the benzene molecules in the headgroup region, but similarly to those between these regions.

The calculated diffusion coefficients for the benzene in the hydrocarbon and the benzene molecules in the bilayer can be explained by analysis of the molecular structure of the systems. The pure hydrocarbon box is homogeneous throughout, and both ends of the hydrocarbon chain are free to rotate. The hydrocarbon chains in the bilayer are bonded at one end but have substantial freedom at the C-14 end, as evidenced by the order parameters (see Figure 2). Studies of the diffusion of penetrants through polymers show that end effects (i.e., number of terminal methyl groups) play an important role in diffusion (Müller-Plathe, 1992; Takeuchi, 1990b) and the presence of more ends increases the rate of diffusion. Note that, as mentioned previously, in the bilayer the terminal methyls are, on average, concentrated at the bilayer center. Thus, although the hydrocarbon chains in the tetradecane box have twice as many free ends as those in the bilayer, at

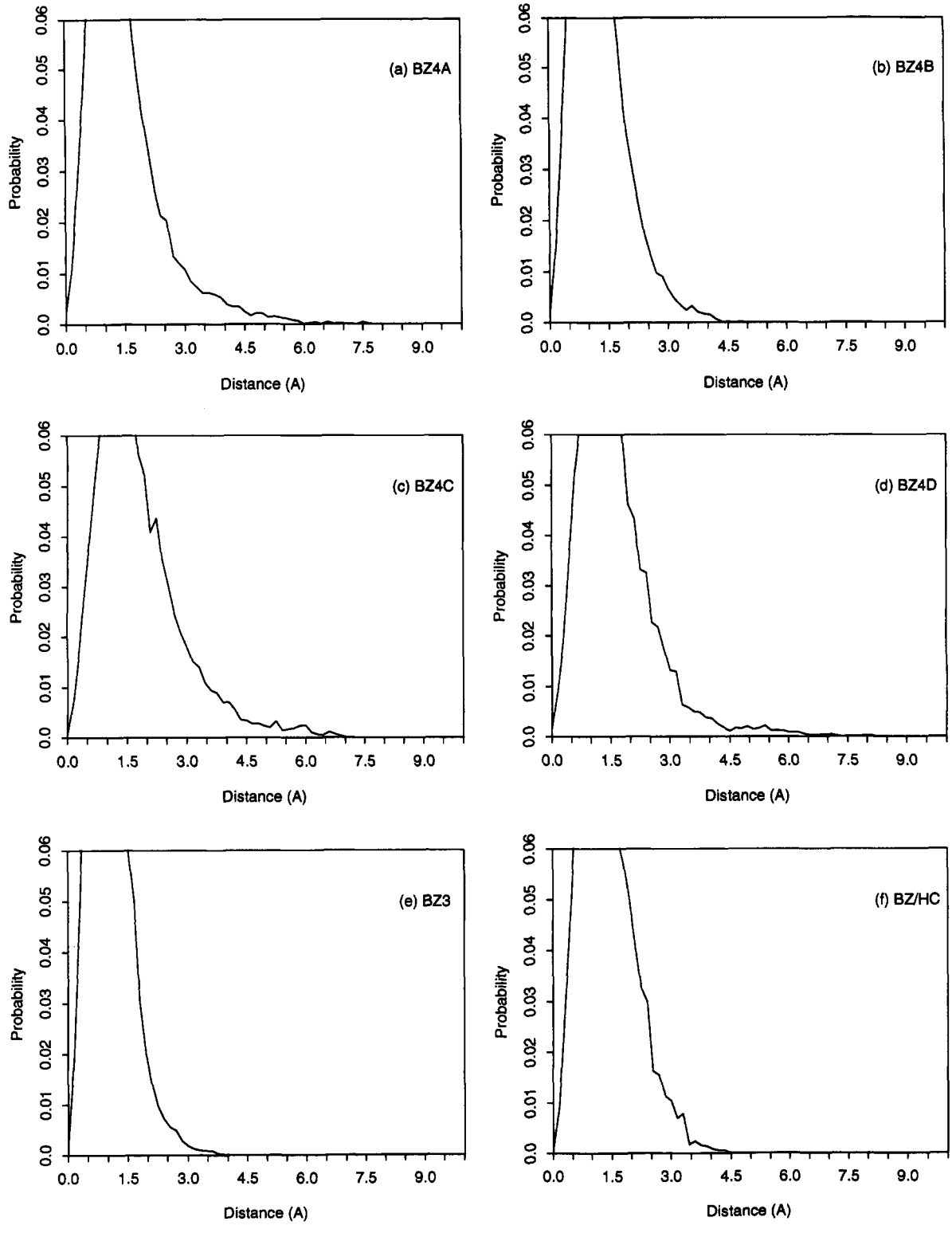

FIGURE 8: Probability distributions of movement over all 10-ps intervals for the simulations (BZ1 and BZ2 are not shown because they were for shorter periods of time): (a) BZ4A; (b) BZ4B; (c) BZ4C; (d) BZ4D; (e) BZ3; (f) benzene in pure hydrocarbon.

the bilayer center the end effects are magnified and solutes in this region experience greater end effects than those in the pure hydrocarbon system (Dill & Flory, 1980). Conversely, in the headgroup region, no end effects at all are present, and the diffusion rates are less than that within the pure hydrocarbon.

The movement of the benzene molecule in the pure hydrocarbon is shown in Figures 7g and 8f. Although it experiences a number of jumps, the jumps are smaller in magnitude than those that are observed for benzene molecules near the center of the bilayer. However, they are larger than those found for benzene molecules nearer the headgroup region. Furthermore, the distribution of movement is qualitatively and quantitatively different from those in the bilayer center and headgroup region. However, it is similar to that of those benzene molecules that reside between the center and the headgroups. For example, in pure hydrocarbon no movements greater than 5 Å are found. Yet the distribution is broader, shorter, and extends into longer distances, more so than does the distribution of BZ3 which resides in the carbonyl region.

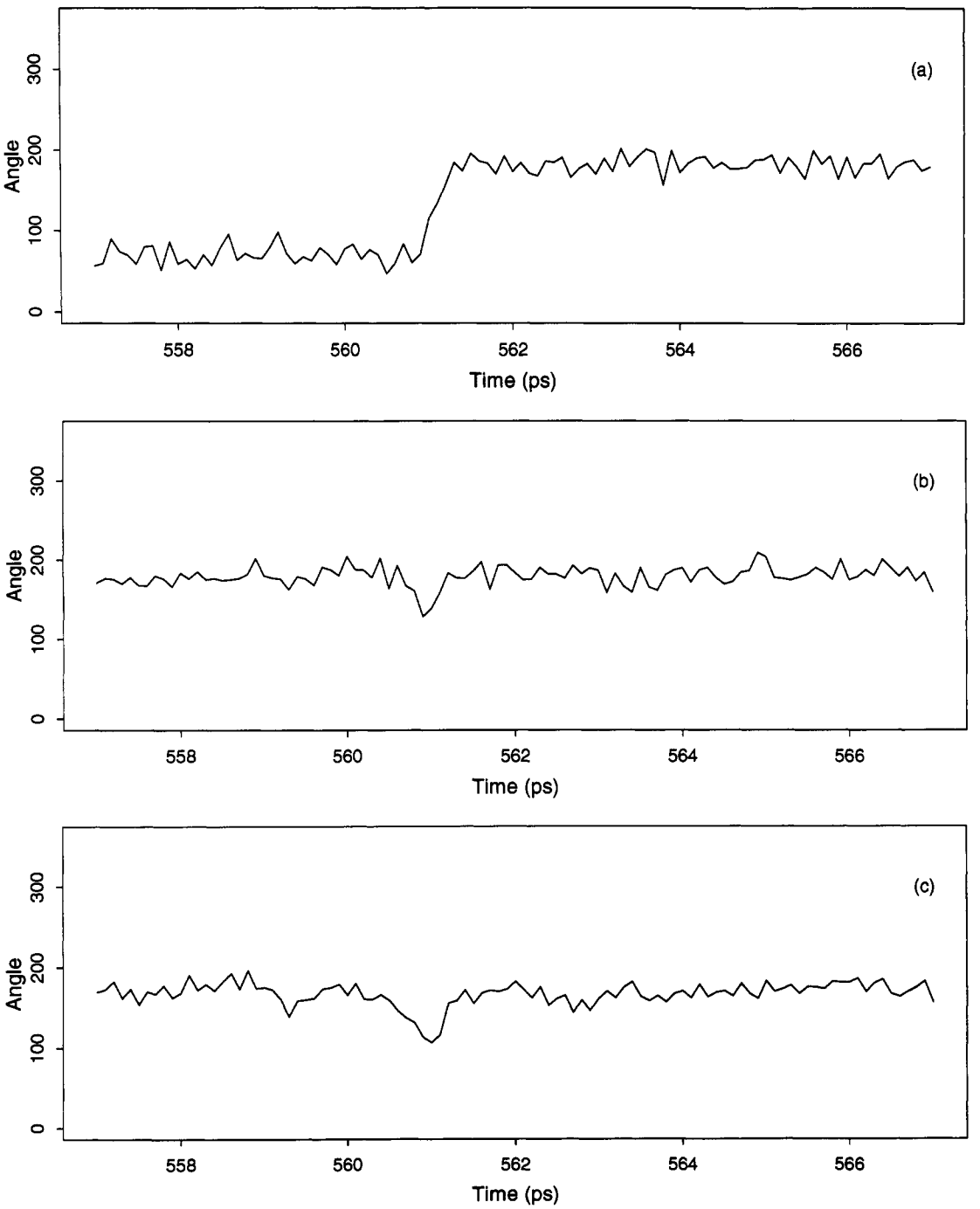

FIGURE 9: Three torsion angles in two chains neighboring a benzene molecule at the time of a jump. The torsion shown in (a) is in one chain and serves to gate the passage of the benzene between two voids. Concerted changes in other torsions on a different chain (b and c) allow the transition in the torsion shown in (a).

In that the density of the tetradecane box is quite close to that of liquid tetradecane, we can liken this one region of the bilayer to pure alkane.

CONCLUSIONS

This study represents the first molecular dynamics simulations of free diffusion of solutes in an atomic-level model of a lipid bilayer. An all-atom representation, including hydrocarbon hydrogen atoms, was used (studies of diffusion in polymers found that a united-atom approach results in diffusion constants in error by almost 2 orders of magnitude). The Lα phase was maintained through a temperature of 320 K and excess solvation of the DMPC bilayer. The simulated models contained over 7100 atoms. Most of the simulations were run for over 1000 ps since 800–900 ps were required for convergence of some properties. The long simulation times allowed reasonable error estimates of the diffusion coefficients of the solutes.

These studies agree with experimental evidence that although small solutes at clinical concentrations do not affect bilayer thickness, they do cause slight perturbations in the order of the hydrocarbon chains. Excellent agreement was found with experimentally derived rotational correlation times and diffusion constants of similar solutes.

As predicted (Marqussee & Dill, 1986), the benzene molecules were free to diffuse throughout the bilayer with no preference for any particular direction. However, the solutes diffused at different rates, depending upon their general

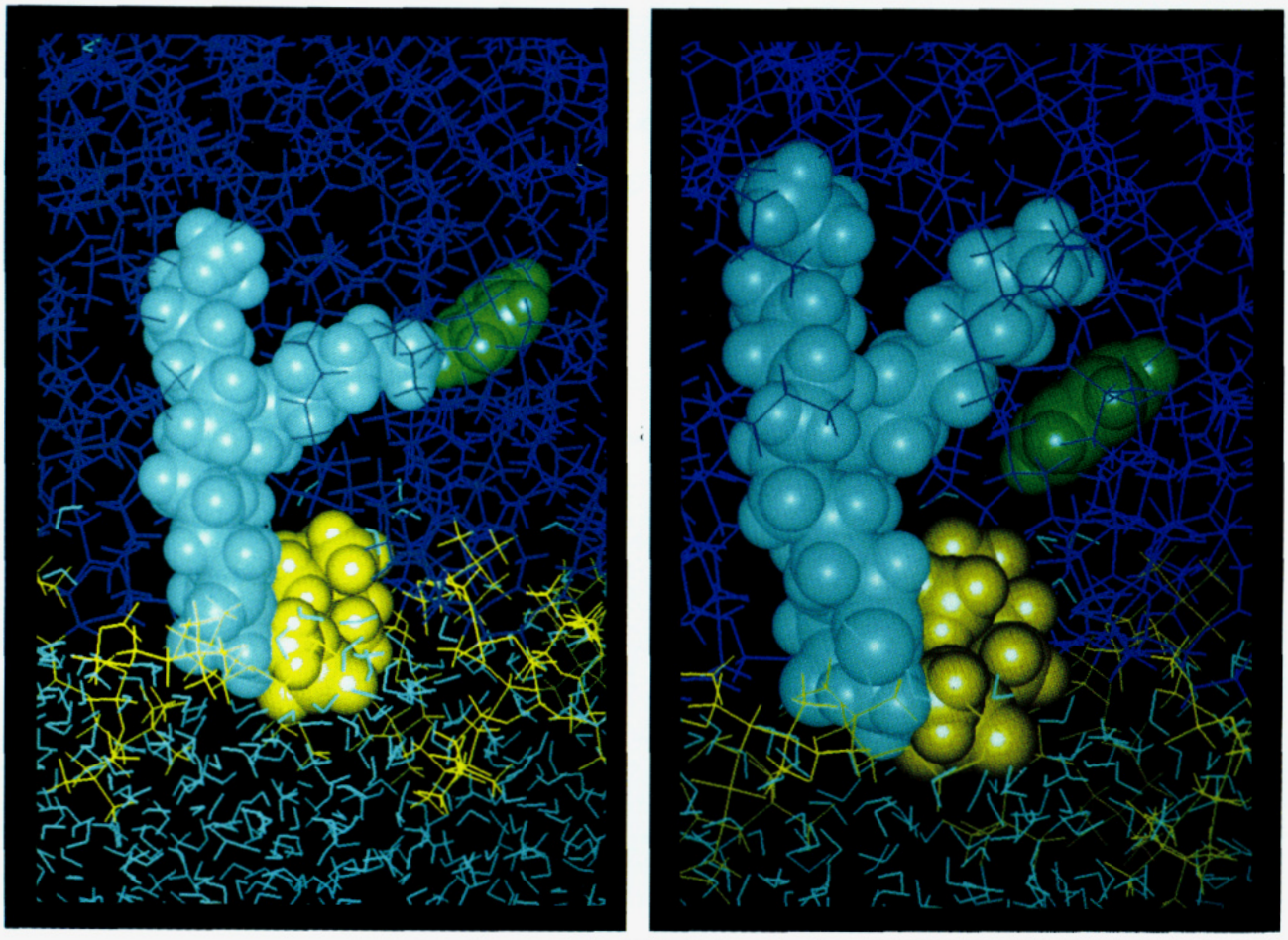

FIGURE 10: Different stages in the jump experienced by BZ4D (a, left) before access to the void blocked by the hydrocarbon chain and (b, right) after a switch in one torsion in the hydrocarbon chain from a gauche rotamer to the trans rotamer moved the chain and allowed the benzene molecule to move from one void to another. The benzene molecules are shown in green, the atoms in the headgroups of the lipid molecules in yellow, the hydrocarbon chains of the lipid molecules in dark blue (except for those of the lipid molecule key to the move, which is light blue), and the water molecules in cyan. The benzene molecule and the lipid molecule directly involved in the jump are shown as CPK models.

location in the bilayer. A gradient of diffusion rates was seen, and those solutes nearer the headgroups diffused 2–3 times slower than those in the center of the bilayer. These results support the theory that headgroup penetration is the rate-determining step in membrane permeability (Dix et al., 1978) and support conclusions that the hydrogen region of the bilayer is not itself homogeneous and cannot be treated as bulk hydrocarbon. Lipid bilayer systems are interfacial, and their properties depend on distance from the lipid/water interface (Dill & Flory, 1981; Marqussee & Dill, 1986; DeYoung & Dill, 1988).

The mechanism of diffusion of solutes occurs in part through jumps between voids, similar to that of small penetrants in soft polymers (Cohen & Turnbull, 1959). The size and frequency of the jumps vary with location in the bilayer. The jumps are larger and more frequent in the low-density bilayer center where the hydrocarbon "end effects" are concentrated than in the densely packed headgroup region. Increased jump size and frequency directly correlate with higher diffusion coefficients.

Current studies include even more detailed investigation to better classify and clarify the mechanism of solute diffusion in different bilayer regions. Diffusion mechanisms might be expected to change with solute size, and studies of solutes both smaller and several times larger are in progress. The electrostatic potential of bilayers plays an active role in membrane structure and function and influences the membrane permeability of small molecules. The effects of solute polarity and its interaction with this potential are also under investigation.

ACKNOWLEDGMENT

The authors thank Malcolm Davis for his assistance in preparing the figures for the manuscript. The authors are indebted to R. Shaginaw, J. Stringer, R. Gopstein, and G. Burnham (BMS High Performing Computer Center) and S. Samuels (BMS Department of Macromolecular Modeling) for orchestrating our Cray Y-MP and Silicon Graphics computing network and providing essential computer support. We also thank J. Novotny and J. Villafranca for encouraging these studies and for critically reviewing the manuscript.

REFERENCES

Alper, H. E., & Levy, R. M. (1989) *J. Chem. Phys. 91*, 1242–1251.

Alper, H. E., Bassolino, D. A., & Stouch, T. R. (1993a) *J. Chem. Phys. 98*, 9798–9807.

Alper, H. E., Bassolino-Klimas, D., & Stouch, T. R. (1993b) *J. Chem. Phys. 99*, 5547–5559.

Ashcroft, R. G., Coster, H. G. L., & Smith, J. R. (1977) *Nature 269*, 819–820.

Berendsen, H. J. C., Postma, J. P. M., van Gunsteren, W. F., & Hermans, J. (1981) *Intermolecular Forces* (Pullman, B., Ed.) pp 331–342, Reidel, Dordrecht, Holland.

Berendsen, H. J. C., Straatsma, J. P. M., van Gunsteren, W. F., DiNola, A., & Haak, J. R. (1984) *J. Chem. Phys. 79*, 926.

Berkowitz, M. L., & Raghaven, K. (1991) *Langmuir 7*, 1042–1044.
Carriere, B., & LeGrimellec, C. (1986) *Biochim. Biophys. Acta 857*, 131–138.
Cohen, B. E. (1975) *J. Membr. Biol. 20*, 235–268.
Cohen, M. H., & Turnbull, D. (1959) *J. Chem. Phys. 31*, 1164.
Damodaran, K. V., Merz, K. M., & Gaber, B. P. (1992) *Biochemistry 31*, 7656–7664.
Dauber-Osguthorpe, P., Roberts, V. A., Osguthorpe, D. J., Wolff, J., Genest, M., & Hagler, A. T. (1988) *Proteins: Struct., Funct., Genet. 4*, 31.
DeYoung, L. R., & Dill, K. A. (1988) *Biochemistry 27*, 5281–5289.
Dill, K. A., & Flory, P. J. (1980) *Proc. Natl. Acad. Sci. U.S.A. 77*, 3115–3119.
Dill, K. A., & Flory, P. J. (1981) *Proc. Natl. Acad. Sci. U.S.A. 78*, 676–680.
Dix, J. A., Kivelson, D., & Diamond, J. M. (1978) *J. Membr. Biol. 40*, 315–342.
Edholm, O., & Johansson, J. (1987) *Eur. Biophys. J. 14*, 203–209.
Edholm, O., Berendsen, H. J. C., & van der Ploeg, P. (1983) *Mol. Phys. 48*, 379–388.
Egberts, E. (1988) Molecular Dynamics Simulation of Multibilayer Membranes, Ph.D. Thesis, Rijksuniveriteit, Groningen, The Netherlands.
Egberts, E., & Berendsen, H. J. C. (1988) *J. Chem. Phys. 89*, 3718–3732.
Elber, R., & Karplus, M. (1990) *J. Am. Chem. Soc. 112*, 9161–9175.
Elliot, J. R., Murrell, R. D., & Haydon, D. A. (1987) *J. Membr. Biol. 95*, 143–149.
Finkelstein, A. (1976) *J. Gen. Physiol. 68*, 137–143.
Franks, N. P. (1976) *J. Mol. Biol. 100*, 345–358.
Franks, N. P., & Lieb, W. R. (1979) *J. Mol. Biol. 133*, 469–500.
Franks, N. P., & Lieb, W. R. (1981) *Nature 292*, 248–251.
Hagler, A. T., Lifson, S., & Dauber, P. (1979) *J. Am. Chem. Soc. 101*, 5122.
Haydon, D. A., Hendry, B. M., Levinson, S. R., & Requena, J. (1977) *Nature 268*, 356–358.
Hianik, T., Palackova, A., & Palackova, J. (1990) *Gen. Physiol. Biophys. 9*, 267–280.
Hubbell, W. L., & McConnell, H. M. (1971) *J. Am. Chem. Soc. 93*, 314.
Jacobs, R. E., & White, S. H. (1984) *J. Am. Chem. Soc. 106*, 915–920.
Jonsson, B., Edholm, O., & Teleman, O. (1986) *J. Chem. Phys. 85*, 2263–2271.
Ladbrooke, B. D., & Chapman, D. (1969) *Chem. Phys. Lipids 3*, 304.
Lieb, W. R., & Stein, W. D. (1969) *Nature 224*, 240–243.
Lieb, W. R., & Stein, W. D. (1971) *Curr. Top. Membr. Transp. 2*, 1–39.
Marqussee, J. A., & Dill, K. A. (1986) *J. Chem. Phys. 85*, 434–444.
McKinnon, S. J., Whittenburg, S. L., & Brooks, B. (1992) *J. Am. Chem. Soc. 96*, 10497–10506.
Müller-Plathe, F. (1991) *J. Chem. Phys. 94*, 3192–3199.
Müller-Plathe, F. (1992) *J. Chem. Phys. 96*, 3200–3205.
Müller-Plathe, F., Rogers, S. C., & van Gunsteren, W. F. (1992) *Chem. Phys. Lett. 199*, 237–243.
Overton, E. (1899) *Vierteljahrsschr. Naturforsch. Ges. Zuerich 44*, 88–135.
Pastor, R. W., Venable, R. M. & Karplus, M. (1991) *Proc. Natl. Acad. Sci. U.S.A. 88*, 892–896.
Raghaven, K., Reddy, M. R., & Berkowitz, M. L. (1992) *Langmuir 8*, 233–240.
Ryckaert, J.-P., & Klein, M. L. (1986) *J. Chem. Phys. 85*, 1613–1620.
Rychaert, J. P., Mc Donald, I. R., & Klein, M. L. (1989) *Mol. Phys. 67*, 957–979.
Scott, H. L. (1986) *Biochemistry 25*, 6122–6126.
Scott, H. L., & Kalaskar, S. (1989) *Biochemistry 28*, 3687.
Seelig, A., & Seelig, J. (1974) *Biochemistry 13*, 4839.
Seelig, J., & Seelig, A. (1980) *Q. Rev. Biophys. 13*, 19–61.
Seeman, P. (1972) *Pharmacol. Rev. 24*, 583–655.
Smith, P. E., & Pettitt, B. M. (1991) *J. Chem. Phys. 95*, 8430.
Sok, R. M., Berendsen, H. J. C., & van Gunsteren, W. F. (1992) *J. Chem. Phys. 96*, 4699–4704.
Sonnenburg, J., Gao, J., & Weiner, J. H. (1990) *Macromolecules 23*, 4653–4657.
Stouch, T. R. (1993) *Mol. Simul. 10*, 317–345.
Stouch, T. R., Ward, K. B., Altieri, A., & Hagler, A. T. (1991) *J. Comput. Chem. 12*, 1033.
Stouch, T. R., Alper, H. E., & Bassolino, D. (1993) *Int. J. Supercomput. Appl.* (in press).
Takeuchi, H. (1990a) *J. Chem. Phys. 93*, 2062–2067.
Takeuchi, H. (1990b) *J. Chem. Phys. 93*, 4490–4491.
Takeuchi, H., & Okazaki, K. (1990) *J. Chem. Phys. 92*, 5643–5652.
Trauble, H. (1971) *J. Membr. Biol. 4*, 193–208.
Turner, G. L., & Oldfield, E. (1979) *Nature 277*, 669–670.
Van der Ploeg, P., & Berendsen, H. J. C. (1983) *Mol. Phys. 49*, 233–248.
Verkhivker, G., Elber, R., & Gibson, Q. (1992) *J. Am. Chem. Soc. 114*, 7866–7878.
Verlet, L. (1967) *Phys. Rev. 159*, 98.
Walter, A., & Gutknecht, J. (1984) *J. Membr. Biol. 77*, 255–264.
Walter, A., & Gutknecht, J. (1986) *J. Membr. Biol. 90*, 207–217.
Watanabe, K., Ferrario, M., & Klein, M. (1988) *J. Chem. Phys. 92*, 818–821.
Wendoloski, I., J., Kimatian, S. J., Schutt, C. E., & Salemme, F. R. (1989) *Science 243*, 636–638.
Williams, D. E. (1967) *J. Chem. Phys. 47*, 4680.
Williams, D. E., & Stouch, T. R. (1993) *J. Comput. Chem. 14*, 1066–1076.